iScience

CellPress
OPEN ACCESS

Article

Dynamic Capture and Release of Endoplasmic Reticulum Exit Sites by Golgi Stacks in Arabidopsis

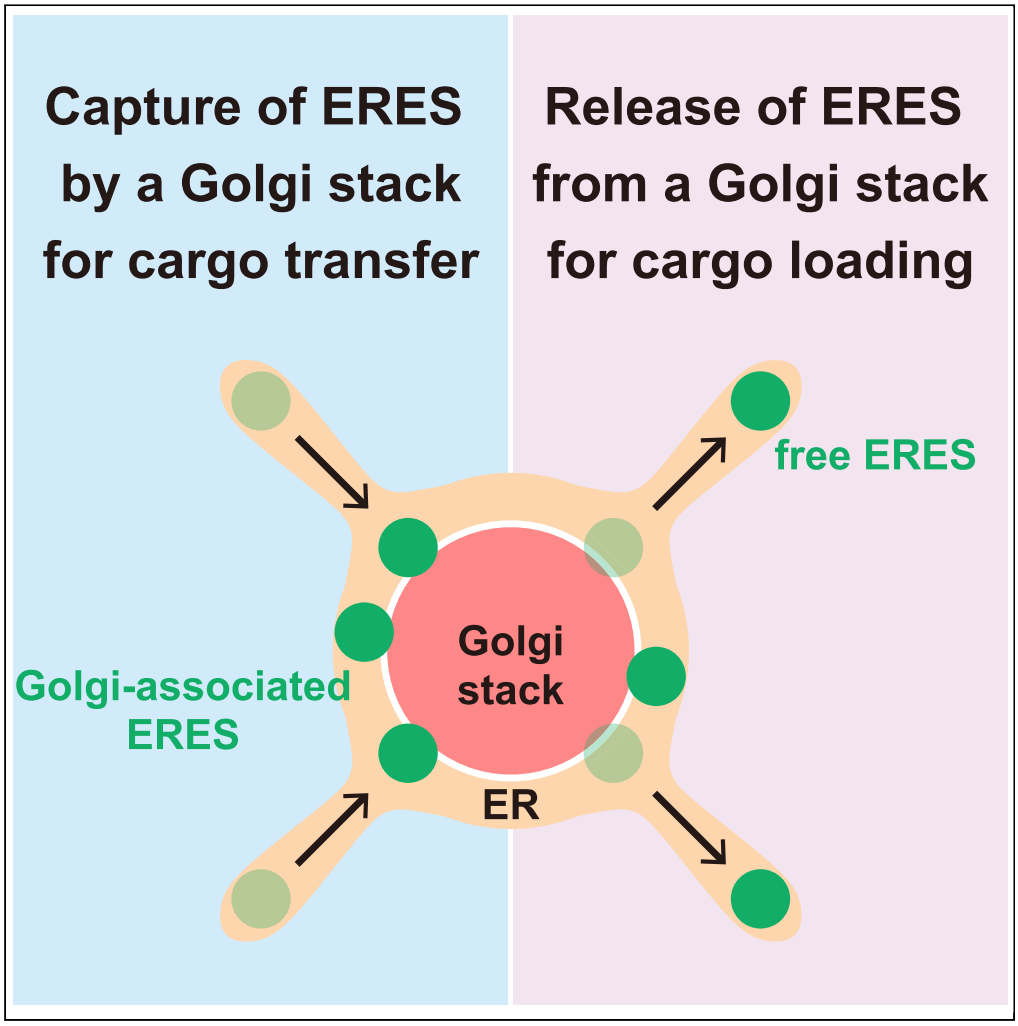

Junpei Takagi, Yoshitaka Kimori, Tomoo Shimada, Ikuko Hara-Nishimura

ihnishi@gr.bot.kyoto-u.ac.jp

HIGHLIGHTS

VAEM images show dynamic behavior of minimal punctate ERESs

Most of punctate ERESs are distributed on the ER network tubes

Several punctate ERESs contact with a Golgi stack in an ER network cavity

ERESs are dynamically captured and released by Golgi stacks

Takagi et al., iScience 23, 101265
July 24, 2020 © 2020 The Author(s).
https://doi.org/10.1016/j.isci.2020.101265

iScience

CellPress
OPEN ACCESS

Article

Dynamic Capture and Release of Endoplasmic Reticulum Exit Sites by Golgi Stacks in Arabidopsis

Junpei Takagi,[1] Yoshitaka Kimori,[2] Tomoo Shimada,[3] and Ikuko Hara-Nishimura[1,4,*]

SUMMARY

Protein transport from the endoplasmic reticulum (ER) to Golgi stacks is mediated by the coat protein complex COPII, which is assembled at an ER subdomain called ER exit site (ERES). However, the dynamic relationship between ERESs and Golgi stacks is unknown. Here, we propose a dynamic capture-and-release model of ERESs by Golgi stacks in *Arabidopsis thaliana*. Using variable-angle epifluorescence microscopy with high-temporal-resolution imaging, COPII-component-bound ERESs were detected as punctate structures with sizes of 300–500 nm. Some punctate ERESs are distributed on ER tubules and sheet rims, whereas others gather around a Golgi stack in an ER-network cavity to form a beaded-ring structure. Free ERESs that wander into an ER cavity are captured by a Golgi stack in a cytoskeleton-independent manner. Then, they are released by the Golgi stack for recycling. The dynamic ERES cycling might contribute to efficient transfer of *de novo* synthesized cargo proteins from the ER to Golgi stacks.

INTRODUCTION

Protein transport from the endoplasmic reticulum (ER) to Golgi stacks is mediated by the coat protein complex II (COPII) machinery (Brandizzi and Barlowe, 2013). COPII vesicles are formed as follows: (1) The guanine nucleotide exchange factor SEC12 activates GTPase SAR1 (Barlowe and Schekman, 1993; Nakano and Muramatsu, 1989), (2) GTP-bound Sar1 recruits the inner-coat-protein complex SEC23/SEC24 to the ER membrane (Bi et al., 2002), (3) SEC24 functions in the selective loading of cargo proteins by recognizing their sorting signals (Miller et al., 2003), and then (4) SAR1-SEC23/SEC24-cargo complexes are polymerized by the outer-coat-protein complex SEC13/SEC31 to form COPII-coated vesicles (Bi et al., 2007; Stagg et al., 2008). COPII-coat-protein assembly occurs at ER subdomains called ER exit sites (ERESs) (Brandizzi and Barlowe, 2013), in which SEC16 functions as a scaffold and regulatory protein to facilitate the assembly (Connerly et al., 2005; Ivan et al., 2008; Kung et al., 2012; Watson et al., 2006; Yorimitsu and Sato, 2012). SEC16 and the plant homolog MAG5 are localized at ERESs but are not included in the COPII-coat complex (Takagi et al., 2013; Yorimitsu and Sato, 2012).

COPII vesicles bud off ERESs and then fuse with Golgi stacks to transfer cargo proteins (Brandizzi and Barlowe, 2013). In *Saccharomyces cerevisiae*, in which ERESs are not always located adjacent to Golgi stacks, *cis*-Golgi cisternae transiently come in contact with ERESs for COPII-dependent cargo transfer (Kurokawa et al., 2014). This result emphasizes the need for Golgi-stack contact with ERESs for the accurate transport of cargo proteins. On the other hand, unlike *S. cerevisiae*, ERESs are closely associated with a Golgi stack in various organisms: plants (daSilva et al., 2004; Ito et al., 2012; Takagi et al., 2013), *Drosophila melanogaster* (Ivan et al., 2008; Kondylis and Rabouille, 2003), *Caenorhabditis elegans* (Witte et al., 2011), *Pichia pastoris* (Bevis et al., 2002), and *Trypanosoma brucei* (Sevova and Bangs, 2009). In mammalian cells, ER-Golgi intermediate compartments (ERGICs) are closely localized to ERESs, instead of Golgi stacks forming a complex Golgi ribbon that is distant from ERESs (Hammond and Glick, 2000; Hughes et al., 2009). However, even though many studies have examined ER-Golgi cargo transport, the dynamic relationship between ERESs and Golgi stacks remains unknown.

A significant feature of plant cells is that cytosolic organelles including the ER are confined to a thin region between the plasma membrane and the membrane of a large central vacuole that occupies most of the cell volume. ERESs are distributed in this narrow region, which makes it possible to track their dynamic movements over a broad focal plane of the cell. To track ERESs in real time, we used variable-angle

[1]Faculty of Science and Engineering, Konan University, Kobe 658-8501, Japan

[2]Faculty of Environmental and Information Sciences, Fukui University of Technology, Fukui 910-8505, Japan

[3]Graduate School of Science, Kyoto University, Kyoto 606-8502, Japan

[4]Lead Contact

*Correspondence: ihnishi@gr.bot.kyoto-u.ac.jp

https://doi.org/10.1016/j.isci.2020.101265

This is an open access article under the CC BY license (http://creativecommons.org/licenses/by/4.0/).

epifluorescence microscopy (VAEM), which provides high temporal resolution of events near the plasma membrane of a tissue (Konopka and Bednarek, 2008).

In this study, using VAEM and plant cells, we were able to observe the dynamic capture-and-release process of ERESs by Golgi stacks in *Arabidopsis thaliana*. Imaging of live cells revealed that some punctate ERESs gathered around a Golgi stack to form a beaded-ring structure at an ER network cavity, whereas other punctate ERESs were distributed on ER tubules and ER sheet rims. Real-time imaging with high temporal resolution showed that some punctate ERESs were captured and released by Golgi stacks in a cytoskeleton-independent manner. The present results reveal the dynamic cycling of ERESs responsible for the efficient cargo transfer from the ER to Golgi stacks.

RESULTS

VAEM Images Reveal Minimal Punctate ERESs, Some of Which Appear to Form Beaded Rings

To identify ERESs, we used the ERES marker MAG5 labeled with GFP in a *MAG5*-deficient mutant under control of the *MAG5* promoter (Takagi et al., 2013). MAG5/SEC16A is a plant homolog of SEC16 that is not present in COPII vesicles (Takagi et al., 2013; Yorimitsu and Sato, 2012). VAEM analysis of the epidermal cell surfaces of cotyledons of the transgenic plants showed a number of MAG5-GFP-positive punctate ERESs with apparent sizes of 300–500 nm (Figure 1A). Most of the MAG5-GFP-positive punctate ERESs were individually distributed throughout the cells (Figure 1A, left). On the other hand, some of the punctate ERESs appeared to form beaded rings with diameters of ~1.5 μm (Figure 1A, middle and right).

Next, we focused on COPII-coat proteins that are assembled at ERESs. Two COPII markers, SEC13A-GFP (Takagi et al., 2013) and YFP-SEC24A (Nakano et al., 2009), were selected because (1) overexpression of SEC24 has no harmful effects on protein transport from the ER (Hanton et al., 2007) and (2) overexpression of SEC24 or SEC13 does not induce ERES formation (Hanton et al., 2009). We investigated transgenic plants that stably expressed each of the COPII markers. VAEM analysis of the epidermal cell surface of cotyledons revealed that each COPII marker labeled punctate structures similar to the MAG5-GFP-positive punctate ERESs (Figures 1B and 1C). To determine the relationship between the COPII-positive punctate structures and punctate ERESs, transgenic plants that stably expressed both YFP-SEC24A and MAG5-mRFP were inspected by VAEM (Figures 1D and S1). Quantitative analysis showed that almost all (~95%) of the YFP-SEC24A-positive punctate structures were labeled with MAG5-mRFP, indicating that COPII-coat proteins assemble on the punctate ERESs (Figure 1E). Hence, the MAG5-positive punctate ERESs can be regarded as a minimal ERES unit at which COPII components are assembled.

Punctate ERESs Occur as Both Golgi-Associated and Golgi-Free ERESs

Positioning ERESs close to Golgi stacks might help to achieve efficient protein transport from the ER to *cis*-Golgi cisternae (Kurokawa et al., 2014). The relationship between the punctate ERESs and *cis*-Golgi cisternae was examined in transgenic plants that stably expressed the ERES marker MAG5-GFP and the *cis*-Golgi marker mCherry-SYP32 (Geldner et al., 2009). SYP32 is a *cis*-Golgi-localized SNARE (soluble *N*-ethylmaleimide sensitive factor attachment protein receptor) protein responsible for vesicle fusion with the target membrane (Uemura et al., 2004). VAEM showed that the beaded ring ERESs structures consisted of a ring of punctate ERESs that surrounded *cis*-Golgi cisternae (Figure 2A, circled). The beaded ring structures correspond to previously identified annular structures of Golgi-associated ERESs that were detected by confocal laser scanning microscopy (Ito et al., 2012; Takagi et al., 2013). On the other hand, most of the free punctate ERESs were distant from *cis*-Golgi cisternae (Figure 2A, arrows). Thus, the cells have two populations of punctate ERESs: a Golgi-associated population and a Golgi-free population. A quantitative analysis of punctate ERES images (Figure S2; see Transparent Methods for details) showed that the number of Golgi-free ERESs is around 1.7 times greater than the number of Golgi-associated ERESs (Figure 2B).

Real-time imaging of the transgenic plants showed that the Golgi stacks rapidly moved within the cell (Figure 2C; Video S1) with velocities similar to those of actin-dependent cytoplasmic streaming (see Figure 5B) (Boevink et al., 1998; Nebenfuhr et al., 1999). Even during their movement, punctate ERESs continued to be associated with Golgi stacks (Figure 2C; Video S1). Similar results were obtained with transgenic plants that stably expressed a COPII marker (SEC13A-GFP or YFP-SEC24A) and the *cis*-Golgi marker mCherry-SYP32 (Figure 2D). Each Golgi stack was accompanied by COPII-positive punctate structures, even while they moved. These results suggest that COPII component-bound punctate ERESs are interacting in some physical way with Golgi stacks.

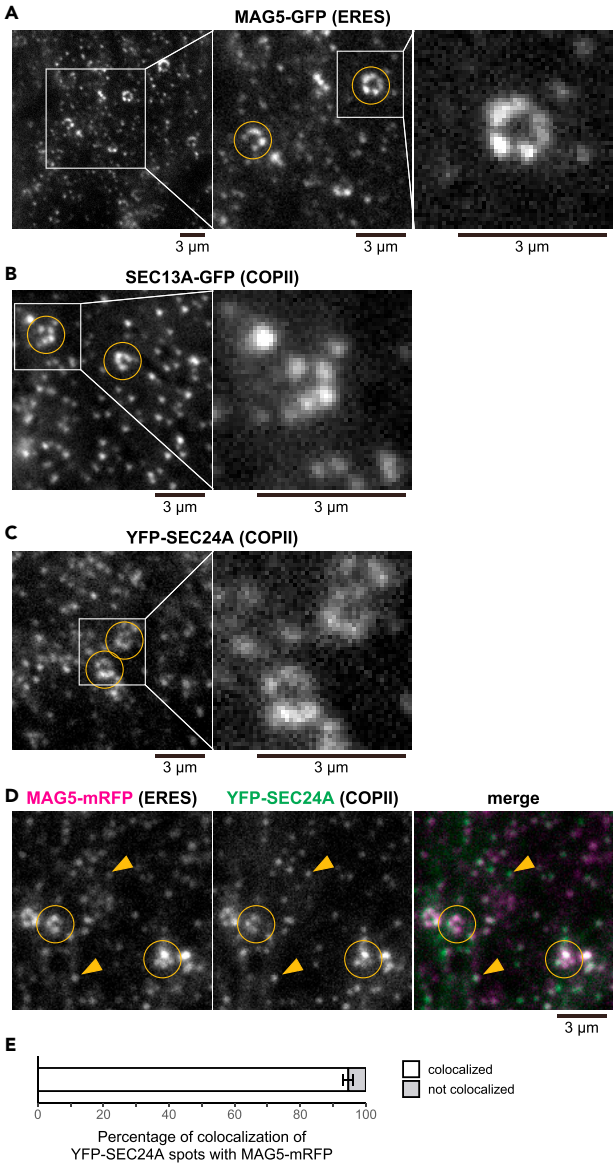

Figure 1. VAEM Images Showing Minimal Punctate ER Exit Sites (ERESs) that Are Accompanied with COPII Components

This figure shows VAEM images of the surface of cotyledon epidermal cells of transgenic plants. Circles indicate beaded rings of punctate ERESs, and arrowheads indicate individually distributed punctate ERESs. Scale bars, 3 μm.

(A) Images of ProMAG5:MAG5-GFP (ERES marker) in *mag5-1* plants. Center panel shows enlarged image of square in left panel; right panel shows enlarged image of square in middle panel.

(B) Images of SEC13A-GFP (COPII marker). Right panel shows enlarged image of square in left panel.

(C) Images of YFP-SEC24A (COPII marker). Right panel shows enlarged image of square in left panel.

(D) Representative images of MAG5-mRFP (ERES marker) and YFP-SEC24A (COPII marker). See also Figure S1 for additional two biological replicates with similar results.

(E) Proportions of YFP-SEC24A (COPII marker)-positive punctate structures that were colocalized and not colocalized with MAG5-mRFP (ERES marker). Error bars represent 95% confidence intervals. n = 1,011 YFP-SEC24A-labeled punctate structures from four biological replicates.

Free Punctate ERESs Are Preferentially Localized to ER Tubules and Sheet Rims

The topological relationship of punctate ERESs with the ER was investigated in transgenic plants that stably expressed the ERES marker MAG5-GFP and the ER marker mCherry-HDEL (Nelson et al., 2007). Free punctate ERESs were widely distributed throughout the ER network (Figure 3A, arrows). Similar results were obtained

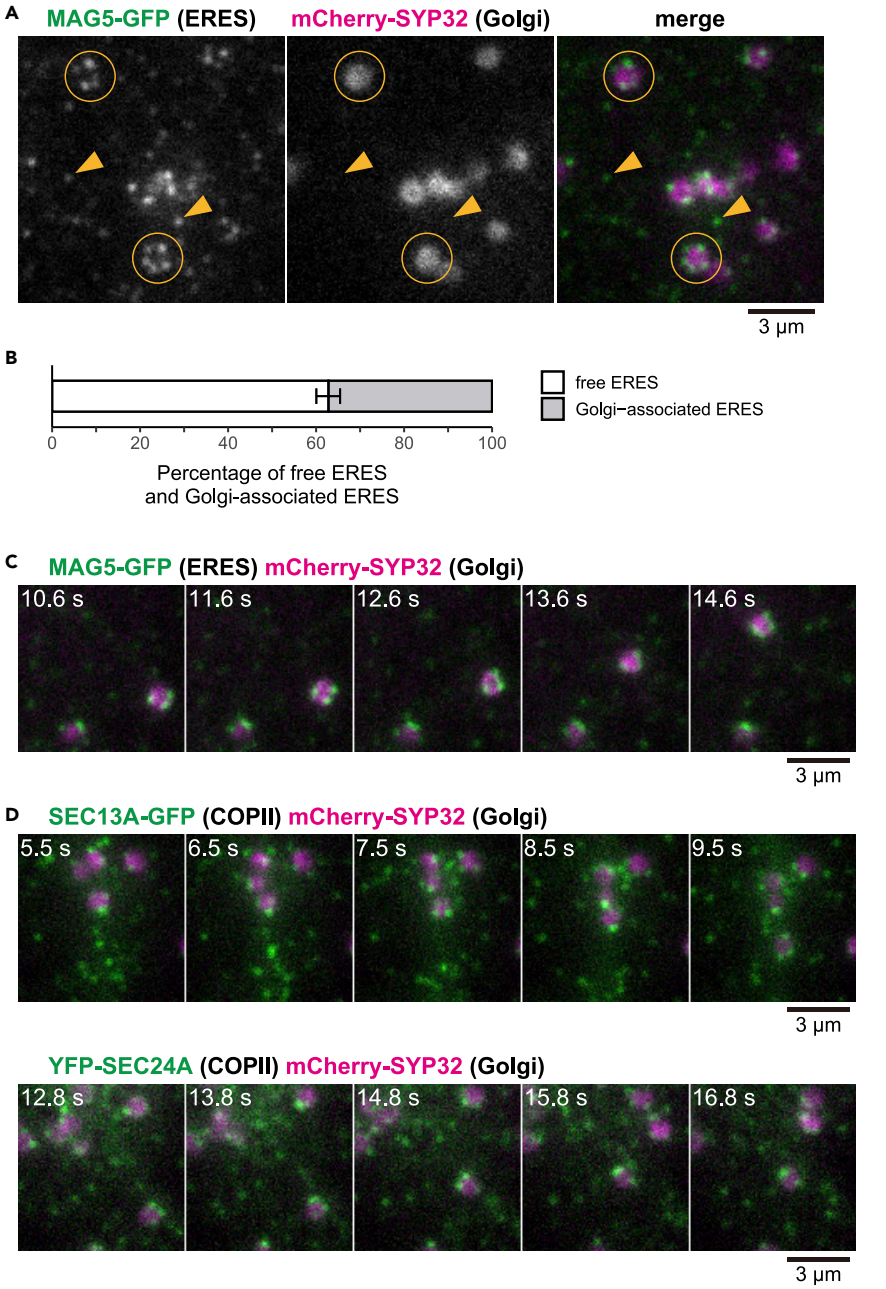

Figure 2. Punctate ERESs Occur as Golgi-Associated and Golgi-Free ERESs

This figure shows VAEM images of the surface of cotyledon epidermal cells of transgenic plants. Scale bars, 3 μm.

(A) Representative images of MAG5-GFP (ERES marker) and mCherry-SYP32 (Golgi marker). Circles indicate beaded rings of ERESs surrounding Golgi stack (Golgi-associated ERESs), and arrowheads indicate individually distributed ERESs free from Golgi stacks (Golgi-free ERESs).

(B) Proportions of Golgi-associated ERESs and Golgi-free ERESs to total MAG5-GFP-labeled punctate ERESs. Error bars represent 95% confidence intervals. n = 1,066 MAG5-GFP-labeled punctate ERESs from five biological replicates. See also Figure S2 for image processing procedures for extraction of Golgi-free ERESs and Golgi-associated ERESs.

(C) Time series of images of MAG5-GFP (ERES marker) and mCherry-SYP32 (Golgi marker) for 4.0 s. See also Video S1 for the original real-time movie.

(D) Time series of images of mCherry-SYP32 (Golgi marker) and each of COPII markers, SEC13A-GFP (upper panels) and YFP-SEC24A (lower panels), for 4.0 s.

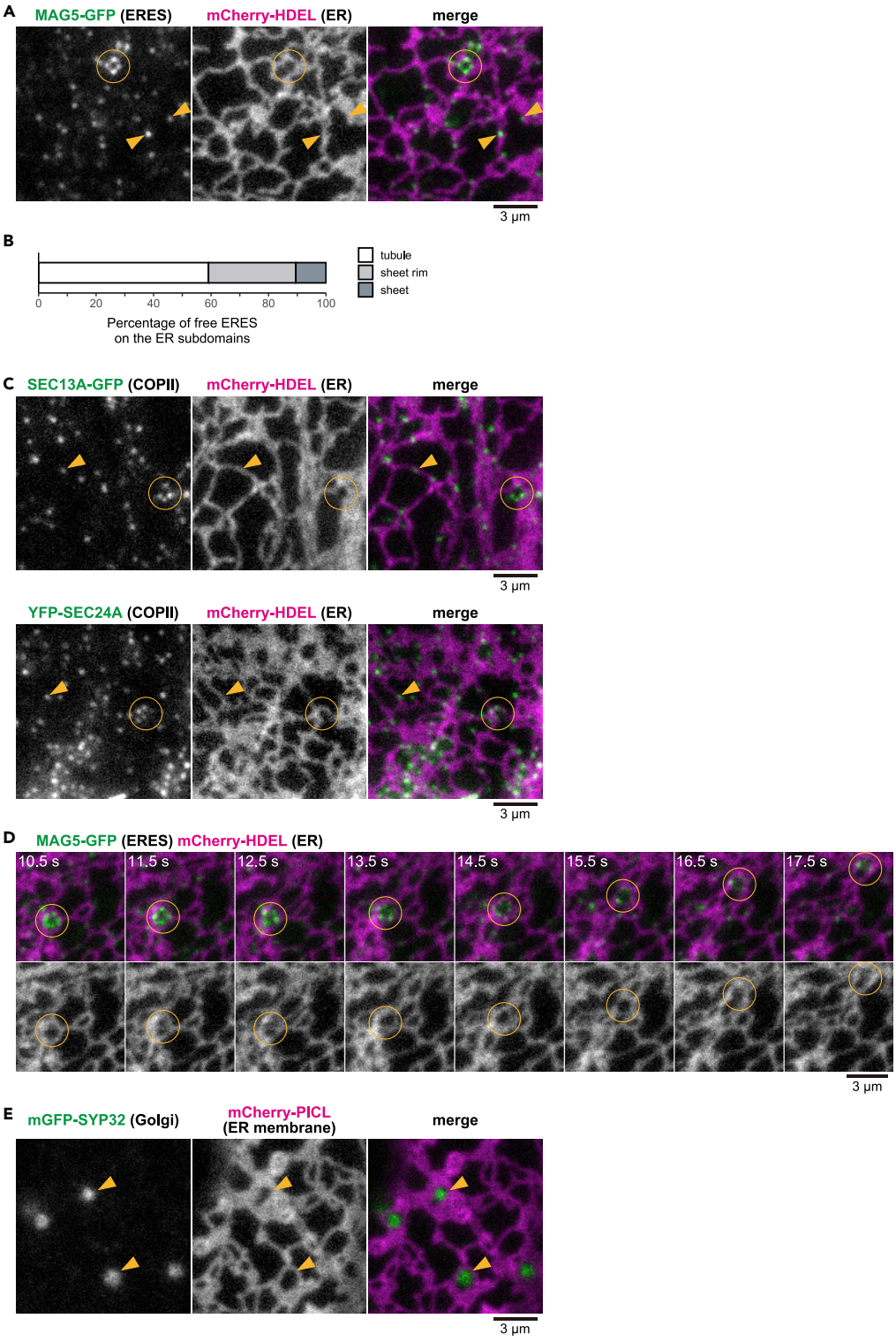

Figure 3. Golgi-Free ERESs Are Preferentially Localized to ER Tubules and Sheet Rims, whereas Golgi-Associated ERESs Are Localized on ER Membranes that Form ER-Network Cavities

This figure shows VAEM images of the surface of cotyledon epidermal cells of transgenic plants. Circles indicate beaded rings of ERESs (Golgi-associated ERESs). Scale bars, 3 μm.

Figure 3. *Continued*
(A) Representative images of MAG5-GFP (ERES marker) and mCherry-HDEL (ER marker) in the same field. Arrowheads indicate individually distributed ERESs (Golgi-free ERESs).
(B) Proportional distribution of Golgi-free ERESs on each of ER subdomains (ER tubule, ER-sheet rim, and ER sheet) to total Golgi-free ERESs. $n = 856$ Golgi-free ERESs from five biological replicates. See also Figure S3 for image processing procedures for extraction of the ER subdomains and Golgi-free ERESs.
(C) Images of mCherry-HDEL (ER marker) and each of COPII markers, SEC13A-GFP (upper panels) and YFP-SEC24A (lower panels). Arrowheads indicate individually distributed ERESs (Golgi-free ERESs).
(D) Time series of images of MAG5-GFP (ERES marker) and mCherry-HDEL (ER marker) for 7.0 s. Merged images (upper) and single-labeled images of mCherry-HDEL (lower) are shown. See also Video S2 for the original real-time movie.
(E) Images of mGFP-SYP32 (Golgi marker) and mCherry-PICL (ER membrane marker). Note that Golgi stacks are localized to the ER cavities (arrowheads).

with COPII-markers (SEC13A-GFP and YFP-SEC24A) (Figure 3C, circled). The ER network is composed of tubules and sheets (Friedman and Voeltz, 2011). To determine the distribution of free punctate ERESs, three typical ER structures (tubules, sheets, and sheet rims; see Figure 6A) were extracted from original fluorescence images of the ER by semi-automatic image processing techniques (Haralick et al., 1987; Kimori, 2011) (Figure S3 and Transparent Methods for details). Approximately 90% of detected free punctate ERESs were on the ER tubules and sheet rims (Figure 3B). Free punctate ERESs are preferentially localized on the curved structures of ER membrane. The free punctate ERESs were associated with COPII markers (Figure 1D), which indicates that COPII vesicles emerge from free punctate ERESs on the ER tubules and sheet rims of the ER network. This is consistent with a previous finding in *Nicotiana benthamiana* that SEC12, which is responsible for initiating COPII vesicle formation, is distributed throughout the ER membrane (daSilva et al., 2004).

Golgi-Associated Punctate ERESs Are Localized on ER Membranes that Form ER Network Cavities

In contrast to preferential localization of free punctate ERESs on the ER tubules and sheet rims, beaded ring-shaped structures labeled with the ERES marker were detected in ER network cavities (Figure 3A, circled). This result indicates that ring-shaped COPII component-bound punctate ERESs, which correspond to Golgi-associated punctate ERESs, are exclusively localized to the ER network cavities. The localization of Golgi-associated punctate ERESs is consistent with previous studies: ERESs have been localized on cup-like structures of the ER in plants (Takagi et al., 2013), on cup-shaped domains of the ER in mammalian cells (Hughes et al., 2009), and on saddle-like structures of the ER in *S. cerevisiae* (Okamoto et al., 2012). Golgi-associated punctate ERESs that were confined to the ER cavities were stable and did not disassemble while they moved in a cytoplasmic streaming-dependent manner (Figure 3D, circled; Video S2). These results suggest that, on the ER membrane forming the cavities, COPII component-bound punctate ERESs are stably associated with Golgi stacks.

To more precisely localize ERESs on the ER membrane, we focused on PICL-TMD, a transmembrane domain of the ER membrane protein PAMP-INDUCED COILED-COIL LIKE (Venkatakrishnan et al., 2013), instead of the ER luminal marker mCherry-HDEL and generated transgenic plants that stably coexpressed the ER membrane marker mCherry-PICL-TMD and the *cis*-Golgi marker mGFP-SYP32. In the cells, Golgi stacks were localized to the ER cavities (Figure 3E). These results indicate that some punctate ERESs are localized on the parts of the ER membranes that form ER cavities.

Cycling of Punctate ERESs between Golgi-Bound and Golgi-Free States

The dynamics of punctate ERESs was examined with high temporal resolution of cells that coexpressed the ERES marker MAG5-GFP and the *cis*-Golgi marker mCherry-SYP32. Some free punctate ERESs were captured by a Golgi stack to directly become punctate ERESs in a Golgi-associated state (Figure 4A; Video S3, left). In another image, a punctate ERES in a Golgi-bound state was released to become a punctate ERES in a free state, which was then captured by another Golgi stack (Figure 4B; Video S3, right). ERES captures and ERES releases by a Golgi stack were each observed about once in 30–40 s (Figure 4C), although the frequencies might be underestimated because of the difficulty of tracking all events by VAEM. Similarly, in the transgenic plants expressing the COPII marker YFP-SEC24A and the *cis*-Golgi marker, a COPII component-bound punctate ERES released by a Golgi stack was captured by another Golgi stack (Figure 4D; Video S4). These results indicate that punctate ERESs cycle between bound and free states. Thus, Golgi stacks might have an ability to dynamically capture and release punctate ERESs.

A MAG5-GFP (ERES) mCherry-SYP32 (Golgi)

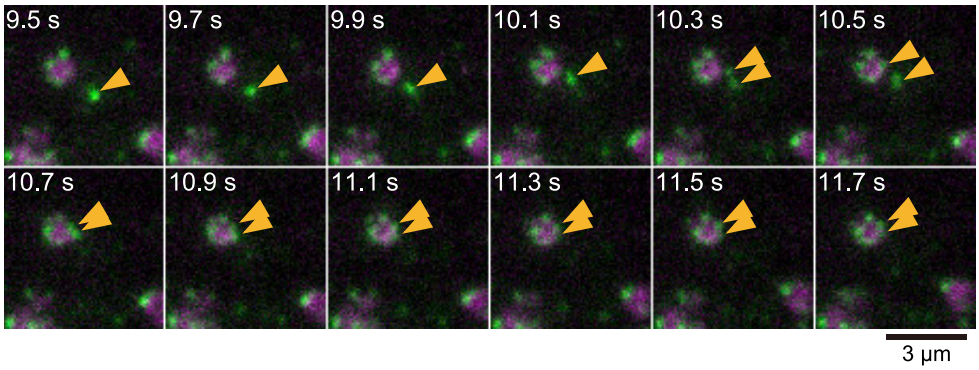

B MAG5-GFP (ERES) mCherry-SYP32 (Golgi)

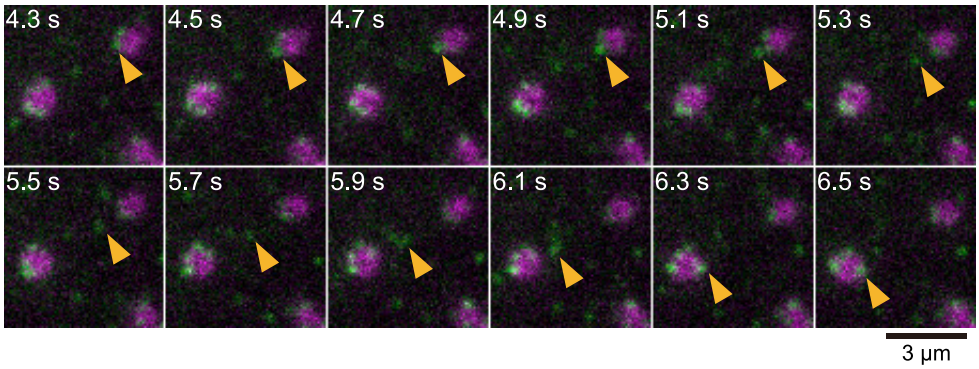

C

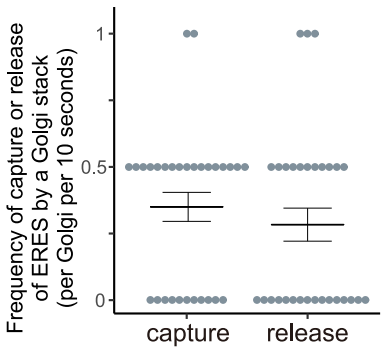

D YFP-SEC24A (COPII) mCherry-SYP32 (Golgi)

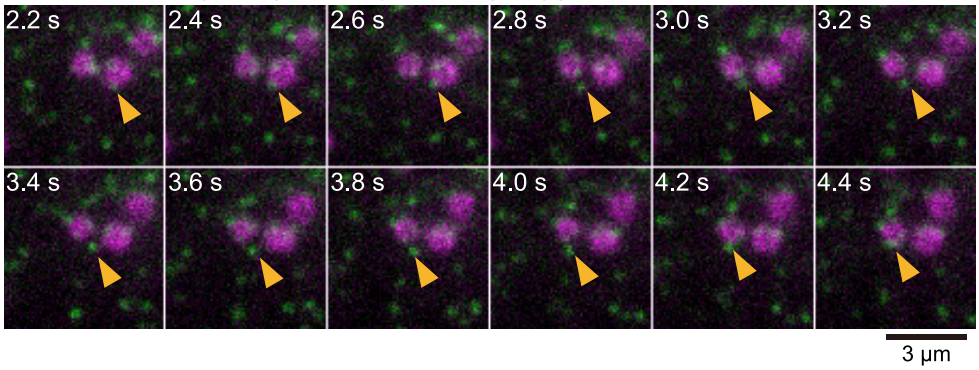

Figure 4. Cycling of Punctate ERESs between Golgi-Bound and Free States

This figure shows VAEM images of the surface of cotyledon epidermal cells of transgenic plants. Scale bars, 3 μm.

(A) Time series of representative images of MAG5-GFP (ERES marker) and mCherry-SYP32 (Golgi marker) for 2.2 s. Arrowheads indicate punctate ERESs being captured by a Golgi stack. See also Video S3 (left) for the original real-time movie.

(B) Time series of representative images of MAG5-GFP (ERES marker) and mCherry-SYP32 (Golgi marker) for 2.2 s. Arrowheads indicate a punctate ERES being released by a Golgi stack and then captured by another Golgi stack. See also Video S3 (right) for the original real-time movie.

(C) Frequencies of the events of capture and release of punctate ERESs for 10 s by a single Golgi stack. Data are represented as mean ± SEM (n = 30 Golgi stacks from 10 biological replicates).

(D) Time series of representative images of YFP-SEC24A (COPII marker) and mCherry-SYP32 (Golgi marker) for 2.2 s. Arrowheads indicate a punctate ERES being released by a Golgi stack and then captured by another Golgi stack. See also Video S4 for the original real-time movie.

Both Golgi stacks (Boevink et al., 1998; Nebenfuhr et al., 1999) and ER strands (Ueda et al., 2010) have been observed to move along cytoplasmic streaming in a cytoskeleton-dependent manner. On the other hand, ER-to-Golgi protein transport does not depend on actin or microtubules (the components of the cytoskeleton) (Brandizzi et al., 2002). To examine the involvement of the cytoskeleton in the cycling of punctate ERESs, transgenic plants were treated with a mixture of an actin-depolymerizing reagent (latrunculin B) and a microtubule-depolymerizing reagent (oryzalin). In the control cells treated with the solvent dimethyl sulfoxide, punctate ERESs showed directional movements along cytoplasmic streaming and random movements similar to Brownian motion (Figure 5A, upper; Video S5, left). Fluorescence particles corresponding to individual Golgi stacks, Golgi-associated ERESs, and free ERESs were tracked on the X-Y plane (Figure 5B). When the inhibitors were used, the directional movements of Golgi-associated and free punctate ERESs were completely impaired (Figure 5A, lower; Video S5, right). However, in the same cells treated with the inhibitors, free punctate ERESs randomly moved and reached Golgi stacks to become Golgi-associated punctate ERESs (Figure 5A, lower, arrowheads). Time-coded trajectories of fluorescence particles of free ERESs clearly show they moved randomly (Figure 5C). Hence, Golgi stacks are able to capture punctate ERESs independently of the cytoskeleton (actin filaments and microtubules).

DISCUSSION

Based on the findings with COPII markers, two ER-Golgi transport models have been proposed in plants (Brandizzi, 2018; Ito et al., 2014). In the kiss-and-run model (also called the stop-and-go model or the dock, pluck, and go model) (Nebenfuhr et al., 1999; Staehelin and Kang, 2008; Yang et al., 2005), ERESs are transiently associated with Golgi stacks whose movements have temporarily stopped. However, our observations show that the Golgi-associated punctate ERESs are moving (Figures 2C and 2D). In the secretory unit model, the secretory units are stable architecture composed of ERESs and Golgi stacks, which predominantly functions in the transport to mobile Golgi stacks (daSilva et al., 2004). In this model, Golgi-free ERESs (if any) can be regarded as premature secretory units (Brandizzi, 2018; Robinson et al., 2015). Our observations have a difference from the secretory unit model: dynamic cycling of punctate ERESs between the Golgi-bound and Golgi-free states (Figure 4). A hybrid model that incorporates different features of the kiss-and-run and secretory unit models has been also proposed (Ito et al., 2014) but never demonstrated.

Based on the present findings with an authentic ERES marker (MAG5), we propose a model for the dynamic capture-and-release of ERESs by Golgi stacks (Figure 6) that overcomes these problems. In this model, the capture and release occurs in three steps: (1) punctate ERESs associated with COPII components move around the ER membrane to load *de novo* synthesized cargo proteins, (2) COPII-bound punctate ERESs that wander into an ER cavity are captured by a Golgi stack, and (3) punctate ERESs are released by Golgi stacks for recycling. In *S. cerevisiae*, COPII vesicles bud off from ERESs during transient contact with Golgi cisternae (Kurokawa et al., 2014). Electron microscopy of *A. thaliana* cells showed that more than 95% of COPII vesicles were detected near Golgi stacks (Kang and Staehelin, 2008). These results suggest that COPII vesicles bud and fuse with *cis*-Golgi cisternae to transport cargo proteins in step 2 of our hypothetical model (Figure 6).

In tobacco BY-2 cells treated with brefeldin A, the *cis*-most cisternae of Golgi are not redistributed into the ER and are associated with ERESs (Ito et al., 2012), suggesting that the *cis*-most cisternae of Golgi are better designed for capturing ERESs in plants. At the ER-Golgi interface, TFG complexes link ERESs to ERGIC membranes in mammalian cells (Johnson et al., 2015) and Tango1 contributes to the organization of the ERES-Golgi interface

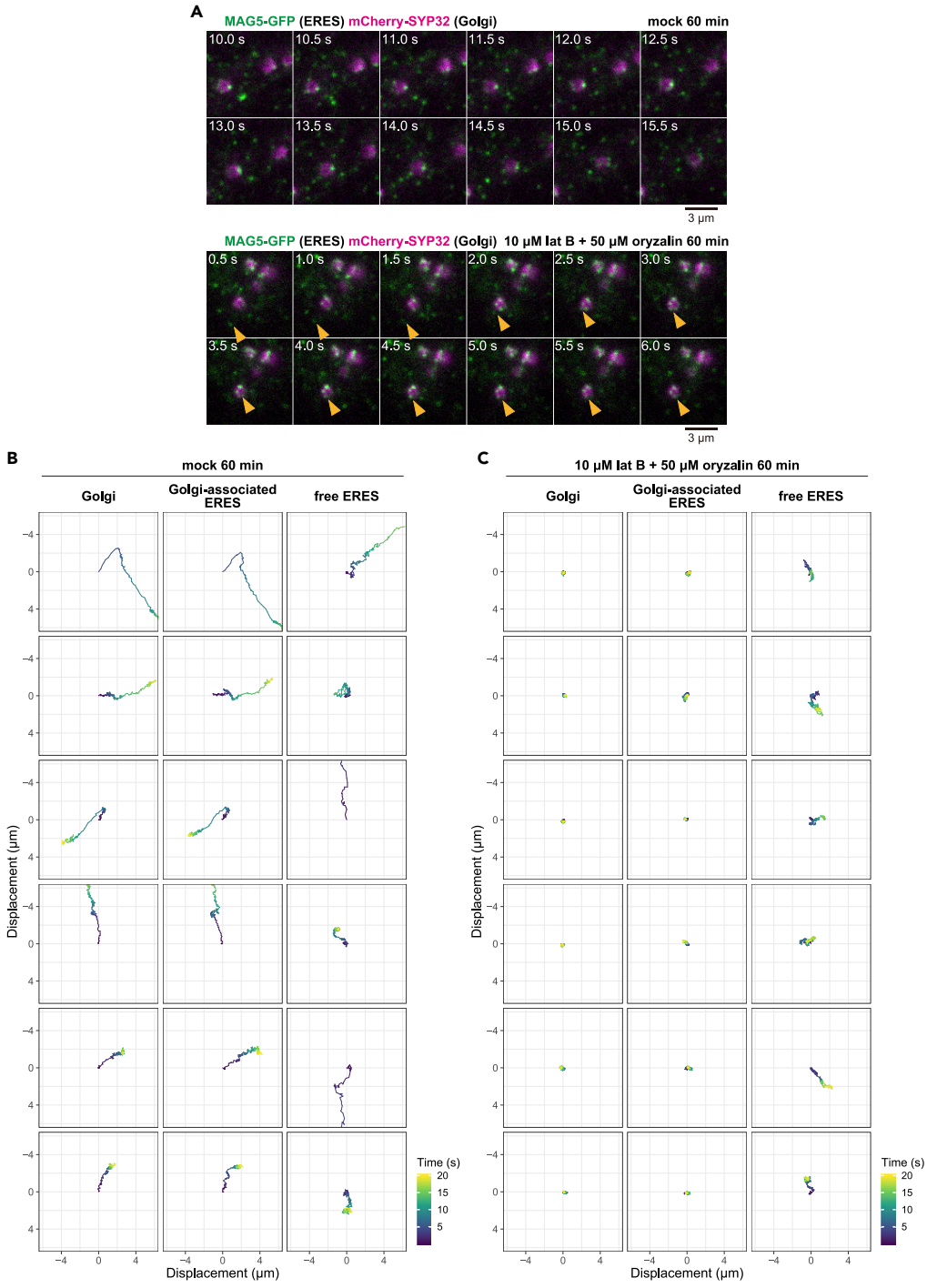

Figure 5. Punctate-ERES Cycling Is Independent of a Cytoskeleton-Dependent Movement

(A) Time series of representative VAEM images of MAG5-GFP (ERES marker) and mCherry-SYP32 (Golgi marker) for 5.5 s. The cotyledon cells were mock-treated (upper panels) or treated with cytoskeleton inhibitors (10 μM latrunculin B and 50 μM oryzalin) (lower panels) for 60 min. See also Video S5 (left and right) for the original real-time movies of mock- and inhibitor-treated cells, respectively. Scale bars, 3 μm.

Figure 5. *Continued*

(B and C) Six example trajectories of fluorescence particles corresponding to each of Golgi stack, Golgi-associated ERES, and free ERES in cotyledon cells that expressed MAG5-GFP (ERES marker) and mCherry-SYP32 (Golgi marker). The cotyledon cells were mock-treated (B) or treated with the cytoskeleton inhibitors (C) for 60 min. Time-coded trajectories of the fluorescence particles were tracked from the center of each two-dimensional lattice. Three biological replicates were performed.

in mammalian cells (Santos et al., 2015) and *D. melanogaster* (Liu et al., 2017). Although *A. thaliana* has no orthologs to TFG and Tango1, their functional homologs might be involved in the process of capture and release of ERESs by Golgi stacks. On the other hand, ERES structures similar to beaded ring-shaped ERESs were also detected in mammalian cells (McCaughey et al., 2016) and in *D. melanogaster* (Liu et al., 2017). Additionally, a simulation of the dynamics of ERESs shows that ERESs randomly move around the ER tubules and are eventually confined by cup-shaped domains of the ER in mammalian cells (Stadler et al., 2018), as in *A. thaliana* (Figure 6). Thus, our model of capture and release of punctate ERESs by Golgi stacks might be applicable to the ER-to-Golgi transport in mammals and in *Drosophila*.

Limitations of the Study

Our study has four limitations. We were unable to (1) verify the dynamics of *individual* COPII vesicles during the budding off of ERESs and fusing with Golgi stack membrane because the close proximity of ERESs and Golgi stacks made it difficult to detect individual COPII vesicles located between them; (2) track cargo-protein transport from the ER to Golgi stacks due to a lack of appropriate pulse-chase type of experimental systems in plant cells; (3) determine the exact frequency of the capture-and-release events of ERESs by a Golgi stack because the ERESs move away from the focal plane and overlap each other during their movement; (4) quantify the changes in signal intensity of COPII on ERESs, due to the ERES movements and a wavelength-dependent control system of laser angles of VAEM.

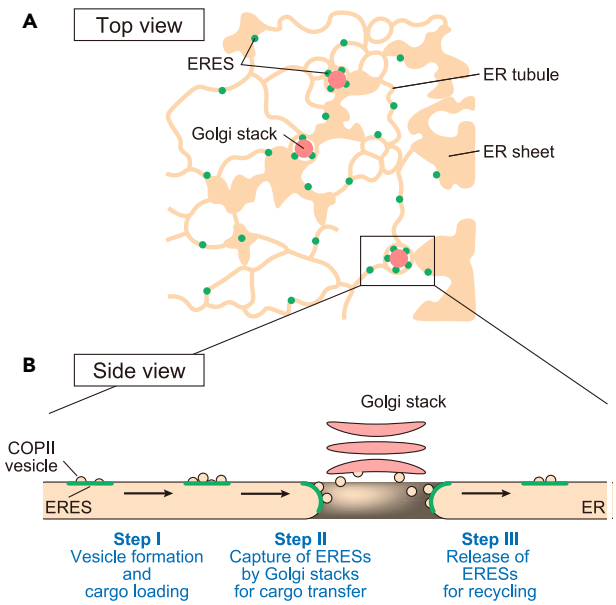

Figure 6. A Hypothetical Model of Capture-and-Release of Punctate ERESs by Golgi Stacks

(A) Top view illustrating the distribution of punctate ERESs (green dots) on the ER network (orange) and Golgi stacks (magenta closed circles). Punctate ERESs exist in both Golgi-free and Golgi-associated states. Most of Golgi-free ERESs are individually distributed on the ER tubules and ER sheet rims, whereas Golgi-associated ERESs are distributed in the ER cavities.

(B) Side view of the ER-Golgi interface illustrates a model for the dynamic capture and release of ERESs by Golgi stacks, in which the ER-Golgi transport occurs in three steps. In Step I, ERESs with forming COPII vesicles (green dots) move around the ER network (orange) to load *de novo* synthesized cargo proteins. In Step II, COPII-bound ERESs are captured by a Golgi stack (pink) in an ER cavity, where COPII vesicles bud from ERESs and fuse with *cis*-Golgi cisternae to transport proteins. In Step III, ERESs are released by Golgi stacks for recycling.

CellPress
OPEN ACCESS

Resource Availability

Lead Contact

Further information and requests for resources and reagents should be directed to and will be fulfilled by the Lead Contact, Ikuko Hara-Nishimura (ihnishi@gr.bot.kyoto-u.ac.jp).

Materials Availability

Materials generated in this study are available from the Lead Contact with a completed Materials Transfer Agreement.

Data and Code Availability

The codes supporting the current study have not been deposited in a public repository because these are parts of further investigation but are available from the corresponding author on request.

METHODS

All methods can be found in the accompanying Transparent Methods supplemental file.

SUPPLEMENTAL INFORMATION

Supplemental Information can be found online at https://doi.org/10.1016/j.isci.2020.101265.

ACKNOWLEDGMENTS

We are grateful to Shoji Segami (National Institute for Basic Biology) and Masayoshi Maeshima (Chubu University), Niko Geldner (University of Lausanne), and Andreas Nebenführ (University of Tennessee) for sharing their materials. This work was supported by Grants-in-Aid for Scientific Research to I.H.-N. (nos. JP22000014 and JP15H05776), to J.T. (nos. JP15J07657 and JP18K14736), and to T.S. (no. JP18K06284) from Japan Society for the Promotion of Science and by the Hirao Taro Foundation of KONAN GAKUEN for Academic Research to I.H.-N.

AUTHOR CONTRIBUTIONS

J.T., T.S., and I.H.-N. conceived the study. J.T. performed all experiments and quantification of dynamics of ERESs and Golgi stacks. Y.K. developed the image analysis algorithms and performed the analyses. J.T., Y.K., T.S., and I.H.-N. analyzed the data and wrote the article.

DECLARATION OF INTERESTS

The authors declare no competing interests.

Received: February 13, 2020
Revised: May 9, 2020
Accepted: June 8, 2020
Published: July 24, 2020

REFERENCES

Barlowe, C., and Schekman, R. (1993). SEC12 encodes a guanine-nucleotide-exchange factor essential for transport vesicle budding from the ER. Nature *365*, 347–349.

Bevis, B.J., Hammond, A.T., Reinke, C.A., and Glick, B.S. (2002). *De novo* formation of transitional ER sites and Golgi structures in *Pichia pastoris*. Nat. Cell Biol. *4*, 750–756.

Bi, X., Corpina, R.A., and Goldberg, J. (2002). Structure of the Sec23/24-Sar1 pre-budding complex of the COPII vesicle coat. Nature *419*, 271–277.

Bi, X., Mancias, J.D., and Goldberg, J. (2007). Insights into COPII coat nucleation from the structure of Sec23.Sar1 complexed with the active fragment of Sec31. Dev. Cell *13*, 635–645.

Boevink, P., Oparka, K., Santa Cruz, S., Martin, B., Betteridge, A., and Hawes, C. (1998). Stacks on tracks: the plant Golgi apparatus traffics on an actin/ER network. Plant J. *15*, 441–447.

Brandizzi, F. (2018). Transport from the endoplasmic reticulum to the Golgi in plants: where are we now? Semin. Cell Dev. Biol. *80*, 94–105.

Brandizzi, F., and Barlowe, C. (2013). Organization of the ER-Golgi interface for membrane traffic control. Nat. Rev. Mol. Cell Biol. *14*, 382–392.

Brandizzi, F., Snapp, E.L., Roberts, A.G., Lippincott-Schwartz, J., and Hawes, C. (2002). Membrane protein transport between the endoplasmic reticulum and the Golgi in tobacco leaves is energy dependent but cytoskeleton independent: evidence from selective photobleaching. Plant Cell *14*, 1293–1309.

Connerly, P.L., Esaki, M., Montegna, E.A., Strongin, D.E., Levi, S., Soderholm, J., and Glick, B.S. (2005). Sec16 is a determinant of transitional ER organization. Curr. Biol. *15*, 1439–1447.

daSilva, L.L., Snapp, E.L., Denecke, J., Lippincott-Schwartz, J., Hawes, C., and Brandizzi, F. (2004). Endoplasmic reticulum export sites and Golgi

bodies behave as single mobile secretory units in plant cells. Plant Cell *16*, 1753–1771.

Friedman, J.R., and Voeltz, G.K. (2011). The ER in 3D: a multifunctional dynamic membrane network. Trends Cell Biol. *21*, 709–717.

Geldner, N., Denervaud-Tendon, V., Hyman, D.L., Mayer, U., Stierhof, Y.D., and Chory, J. (2009). Rapid, combinatorial analysis of membrane compartments in intact plants with a multicolor marker set. Plant J. *59*, 169–178.

Hammond, A.T., and Glick, B.S. (2000). Dynamics of transitional endoplasmic reticulum sites in vertebrate cells. Mol. Biol. Cell *11*, 3013–3030.

Hanton, S.L., Chatre, L., Renna, L., Matheson, L.A., and Brandizzi, F. (2007). De novo formation of plant endoplasmic reticulum export sites is membrane cargo induced and signal mediated. Plant Physiol. *143*, 1640–1650.

Hanton, S.L., Matheson, L.A., Chatre, L., and Brandizzi, F. (2009). Dynamic organization of COPII coat proteins at endoplasmic reticulum export sites in plant cells. Plant J. *57*, 963–974.

Haralick, R.M., Sternberg, S.R., and Zhuang, X. (1987). Image analysis using mathematical morphology. IEEE Trans. Pattern Anal. Mach. Intell. *9*, 532–550.

Hughes, H., Budnik, A., Schmidt, K., Palmer, K.J., Mantell, J., Noakes, C., Johnson, A., Carter, D.A., Verkade, P., Watson, P., et al. (2009). Organisation of human ER-exit sites: requirements for the localisation of Sec16 to transitional ER. J. Cell Sci. *122*, 2924–2934.

Ito, Y., Uemura, T., and Nakano, A. (2014). Formation and maintenance of the Golgi apparatus in plant cells. Int. Rev. Cell Mol. Biol. *310*, 221–287.

Ito, Y., Uemura, T., Shoda, K., Fujimoto, M., Ueda, T., and Nakano, A. (2012). *cis*-Golgi proteins accumulate near the ER exit sites and act as the scaffold for Golgi regeneration after brefeldin A treatment in tobacco BY-2 cells. Mol. Biol. Cell *23*, 3203–3214.

Ivan, V., de Voer, G., Xanthakis, D., Spoorendonk, K.M., Kondylis, V., and Rabouille, C. (2008). *Drosophila* Sec16 mediates the biogenesis of tER sites upstream of Sar1 through an arginine-rich motif. Mol. Biol. Cell *19*, 4352–4365.

Johnson, A., Bhattacharya, N., Hanna, M., Pennington, J.G., Schuh, A.L., Wang, L., Otegui, M.S., Stagg, S.M., and Audhya, A. (2015). TFG clusters COPII-coated transport carriers and promotes early secretory pathway organization. EMBO J. *34*, 811–827.

Kang, B.H., and Staehelin, L.A. (2008). ER-to-Golgi transport by COPII vesicles in *Arabidopsis* involves a ribosome-excluding scaffold that is transferred with the vesicles to the Golgi matrix. Protoplasma *234*, 51–64.

Kimori, Y. (2011). Mathematical morphology-based approach to the enhancement of morphological features in medical images. J. Clin. Bioinform. *1*, 33.

Kondylis, V., and Rabouille, C. (2003). A novel role for dp115 in the organization of tER sites in *Drosophila*. J. Cell Biol. *162*, 185–198.

Konopka, C.A., and Bednarek, S.Y. (2008). Variable-angle epifluorescence microscopy: a new way to look at protein dynamics in the plant cell cortex. Plant J. *53*, 186–196.

Kung, L.F., Pagant, S., Futai, E., D'Arcangelo, J.G., Buchanan, R., Dittmar, J.C., Reid, R.J., Rothstein, R., Hamamoto, S., Snapp, E.L., et al. (2012). Sec24p and Sec16p cooperate to regulate the GTP cycle of the COPII coat. EMBO J. *31*, 1014–1027.

Kurokawa, K., Okamoto, M., and Nakano, A. (2014). Contact of *cis*-Golgi with ER exit sites executes cargo capture and delivery from the ER. Nat. Commun. *5*, 3653.

Liu, M., Feng, Z., Ke, H., Liu, Y., Sun, T., Dai, J., Cui, W., and Pastor-Pareja, J.C. (2017). Tango1 spatially organizes ER exit sites to control ER export. J. Cell Biol. *216*, 1035–1049.

McCaughey, J., Miller, V.J., Stevenson, N.L., Brown, A.K., Budnik, A., Heesom, K.J., Alibhai, D., and Stephens, D.J. (2016). TFG promotes organization of transitional ER and efficient collagen secretion. Cell Rep. *15*, 1648–1659.

Miller, E.A., Beilharz, T.H., Malkus, P.N., Lee, M.C., Hamamoto, S., Orci, L., and Schekman, R. (2003). Multiple cargo binding sites on the COPII subunit Sec24p ensure capture of diverse membrane proteins into transport vesicles. Cell *114*, 497–509.

Nakano, A., and Muramatsu, M. (1989). A novel GTP-binding protein, Sar1p, is involved in transport from the endoplasmic reticulum to the Golgi apparatus. J. Cell Biol. *109*, 2677–2691.

Nakano, R.T., Matsushima, R., Ueda, H., Tamura, K., Shimada, T., Li, L., Hayashi, Y., Kondo, M., Nishimura, M., and Hara-Nishimura, I. (2009). GNOM-LIKE1/ERMO1 and SEC24a/ERMO2 are required for maintenance of endoplasmic reticulum morphology in *Arabidopsis thaliana*. Plant Cell *21*, 3672–3685.

Nebenfuhr, A., Gallagher, L.A., Dunahay, T.G., Frohlick, J.A., Mazurkiewicz, A.M., Meehl, J.B., and Staehelin, L.A. (1999). Stop-and-go movements of plant Golgi stacks are mediated by the acto-myosin system. Plant Physiol. *121*, 1127–1142.

Nelson, B.K., Cai, X., and Nebenfuhr, A. (2007). A multicolored set of *in vivo* organelle markers for co-localization studies in Arabidopsis and other plants. Plant J. *51*, 1126–1136.

Okamoto, M., Kurokawa, K., Matsuura-Tokita, K., Saito, C., Hirata, R., and Nakano, A. (2012). High-curvature domains of the ER are important for the organization of ER exit sites in *Saccharomyces cerevisiae*. J. Cell Sci. *125*, 3412–3420.

Robinson, D.G., Brandizzi, F., Hawes, C., and Nakano, A. (2015). Vesicles versus tubes: is endoplasmic reticulum-golgi transport in plants fundamentally different from other eukaryotes? Plant Physiol. *168*, 393–406.

Santos, A.J., Raote, I., Scarpa, M., Brouwers, N., and Malhotra, V. (2015). TANGO1 recruits ERGIC membranes to the endoplasmic reticulum for procollagen export. Elife *4*, e10982.

Sevova, E.S., and Bangs, J.D. (2009). Streamlined architecture and glycosylphosphatidylinositol-dependent trafficking in the early secretory pathway of African trypanosomes. Mol. Biol. Cell *20*, 4739–4750.

Stadler, L., Speckner, K., and Weiss, M. (2018). Diffusion of exit sites on the endoplasmic reticulum: a random walk on a shivering backbone. Biophys. J. *115*, 1552–1560.

Staehelin, L.A., and Kang, B.H. (2008). Nanoscale architecture of endoplasmic reticulum export sites and of Golgi membranes as determined by electron tomography. Plant Physiol. *147*, 1454–1468.

Stagg, S.M., LaPointe, P., Razvi, A., Gurkan, C., Potter, C.S., Carragher, B., and Balch, W.E. (2008). Structural basis for cargo regulation of COPII coat assembly. Cell *134*, 474–484.

Takagi, J., Renna, L., Takahashi, H., Koumoto, Y., Tamura, K., Stefano, G., Fukao, Y., Kondo, M., Nishimura, M., Shimada, T., et al. (2013). MAIGO5 functions in protein export from Golgi-associated endoplasmic reticulum exit sites in *Arabidopsis*. Plant Cell *25*, 4658–4675.

Ueda, H., Yokota, E., Kutsuna, N., Shimada, T., Tamura, K., Shimmen, T., Hasezawa, S., Dolja, V.V., and Hara-Nishimura, I. (2010). Myosin-dependent endoplasmic reticulum motility and F-actin organization in plant cells. Proc. Natl. Acad. Sci. U S A *107*, 6894–6899.

Uemura, T., Ueda, T., Ohniwa, R.L., Nakano, A., Takeyasu, K., and Sato, M.H. (2004). Systematic analysis of SNARE molecules in Arabidopsis: dissection of the post-Golgi network in plant cells. Cell Struct. Funct. *29*, 49–65.

Venkatakrishnan, S., Mackey, D., and Meier, I. (2013). Functional investigation of the plant-specific long coiled-coil proteins PAMP-INDUCED COILED-COIL (PICC) and PICC-LIKE (PICL) in *Arabidopsis thaliana*. PLoS One *8*, e57283.

Watson, P., Townley, A.K., Koka, P., Palmer, K.J., and Stephens, D.J. (2006). Sec16 defines endoplasmic reticulum exit sites and is required for secretory cargo export in mammalian cells. Traffic *7*, 1678–1687.

Witte, K., Schuh, A.L., Hegermann, J., Sarkeshik, A., Mayers, J.R., Schwarze, K., Yates, J.R., 3rd, Eimer, S., and Audhya, A. (2011). TFG-1 function in protein secretion and oncogenesis. Nat. Cell Biol. *13*, 550–558.

Yang, Y.D., Elamawi, R., Bubeck, J., Pepperkok, R., Ritzenthaler, C., and Robinson, D.G. (2005). Dynamics of COPII vesicles and the Golgi apparatus in cultured *Nicotiana tabacum* BY-2 cells provides evidence for transient association of Golgi stacks with endoplasmic reticulum exit sites. Plant Cell *17*, 1513–1531.

Yorimitsu, T., and Sato, K. (2012). Insights into structural and regulatory roles of Sec16 in COPII vesicle formation at ER exit sites. Mol. Biol. Cell *23*, 2930–2942.

iScience, Volume *23*

Supplemental Information

Dynamic Capture and Release of Endoplasmic Reticulum Exit Sites by Golgi Stacks in Arabidopsis

Junpei Takagi, Yoshitaka Kimori, Tomoo Shimada, and Ikuko Hara-Nishimura

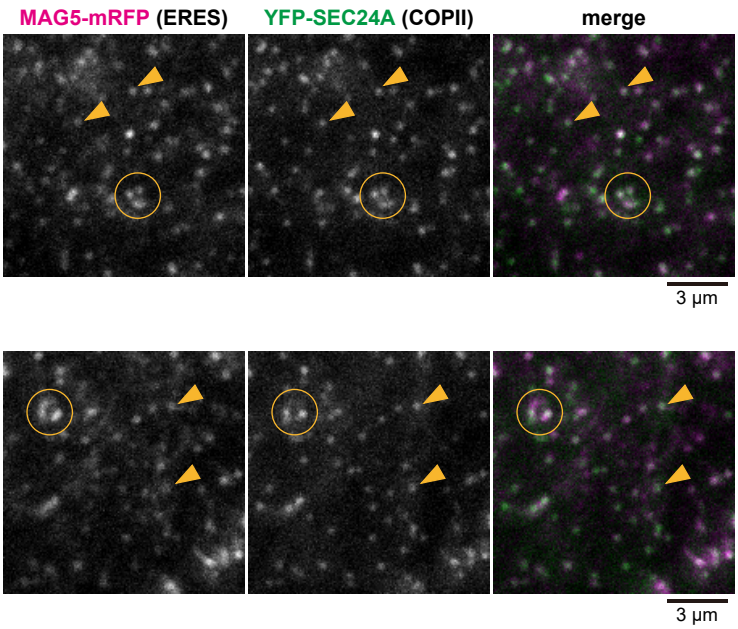

Figure S1. Almost all of YFP-SEC24A-Positive Punctate Structures Are Labeled with MAG5-mRFP, Related to Figure 1D.

Two sets of other representative VAEM images of MAG5-mRFP (ERES marker) and YFP-SEC24A (COPII marker). The surface of cotyledon epidermal cells of transgenic plants was examined. Circles indicate beaded rings of punctate ERESs (Golgi-associated ERESs) and arrowheads indicate individually-distributed punctate ERESs (Golgi-free ERESs). Bars = 3 μm.

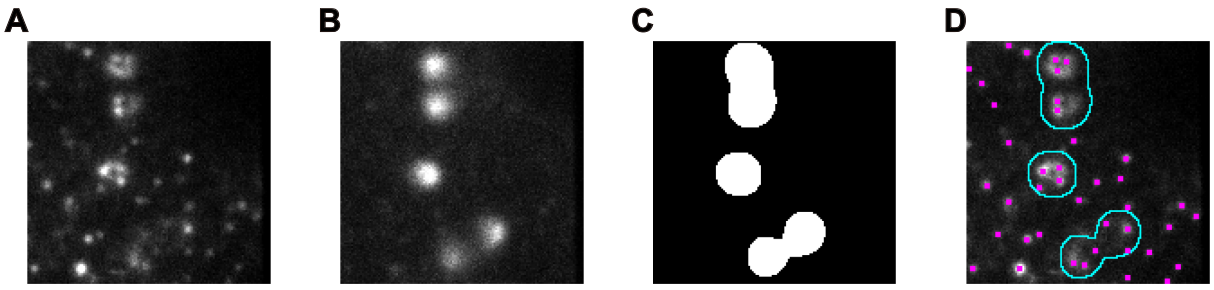

Figure S2. Image Processing Procedures for Extraction Free ERESs and Golgi-Associated ERESs, Related to Figure 2B.

(A) An original image of punctate ERESs.

(B) An original image of Golgi stacks.

(C) Binarized image of (B). The Golgi stack regions are shown in white.

(D) Final image after applying image processing steps. The peaks of the fluorescent spots of ERESs are shown in magenta, and the outlines of the Golgi stack regions are shown in cyan. The ERES spots whose peaks were located in the Golgi stack regions are defined as Golgi-associated ERESs, while the others are free ERESs.

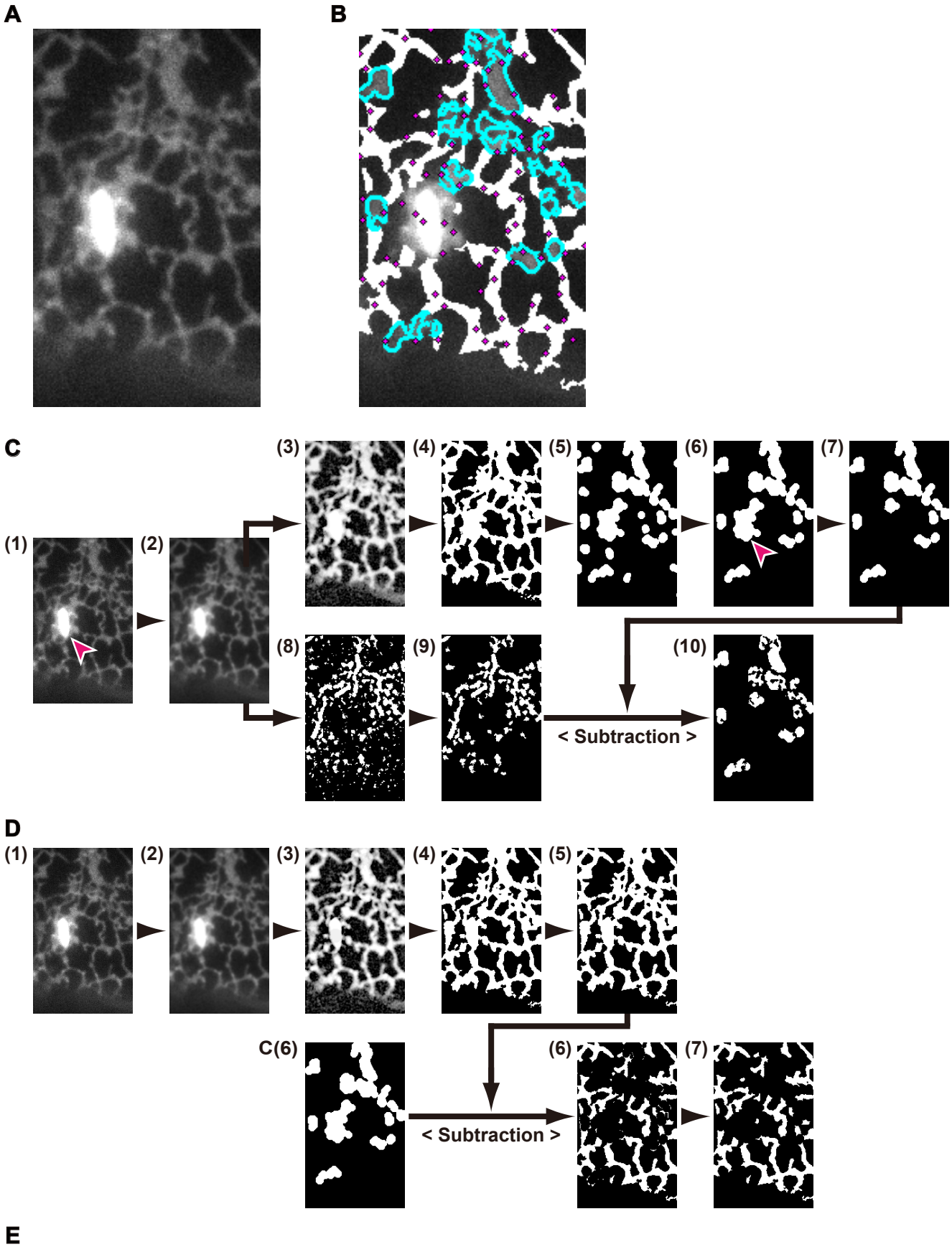
A
B
C
(1)
(2)
(3)
(4)
(5)
(6)
(7)
(8)
(9)
(10)
< Subtraction >
D
(1)
(2)
(3)
(4)
(5)
C(6)
(6)
(7)
< Subtraction >
E
(1)
(2)
(3)
(4)
(5)

Figure S3. Image Processing Procedures for Extraction of the ER Structures and Punctate ERESs, Related to Figure 3B.

(A) An original image.

(B) Final image after applying our proposed image processing steps. The ER tubules are shown in white. The ER sheet rims are shown in cyan, which are defined as the contour of the ER sheet region with a width of three pixels. ERESs are represented in magenta. These structures are superimposed on the original image.

(C-E) Image processing steps for extraction of different ER regions and ERESs.

(C) ER sheet regions. (1) Example of the original image. This image is a partial region of the fluorescent microscopy image. The ER body region is indicated by an arrowhead. (2) The image resulting after Gaussian blurring to remove noise effects. (3) The image resulting after contrast enhancement based on white top-hat transform through rotational morphological processing (RMP). (4) The binarized image using an automatic thresholding method. (5) The image produced after the opening procedure with RMP to remove the ER tubule regions. (6) The resulting image after area opening operation to remove small isolated regions in the image (5). The ER body region, which is indicated by an arrowhead, required manual removal. (7) The image obtained after image processing. (8) The binarized image. Grooves seen in image (2), which are narrow regions with low intensities, were extracted by black top-hat transform through RMP and the resultant image is binarized. (9) The image resulting after area opening operation to remove small isolated regions. (10) The final ER sheet image after the completion of processing. Image (10) is obtained by subtracting image (9) from image (7).

(D) ER tubule regions. (1) An original image. (2) The image produced after Gaussian blurring. (3) The resulting image after white top-hat transform through RMP. (4) Image binarized using an automatic thresholding method. (5) The image resulted after area opening operation to remove small isolated regions. (6) The image resulted from subtracting image C (6) from image (5). (7) The final image showing the extracted ER tubule regions. The image is obtained by removing small, isolated regions present in the image (6).

(E) Free ERES and Golgi-associated ERES regions. (1) An original image. (2) Image produced after Gaussian blurring. (3) The image resulted after closing through RMP to connect adjacent ERESs smoothly. (4) The binarized image using an automatic thresholding method. (5) The image resulted after manual selection of Golgi-associated ERES regions. Fluorescence peaks were extracted from image (1) using the find maxima tool in ImageJ, and peaks other than those within the Golgi-associated ERES regions were defined as free ERESs.

Transparent Methods

Key Resource Table

REAGENT or RESOURCE	SOURCE	IDENTIFIER
Bacterial and Virus Strains		
A. tumefaciens GV3101	N/A	N/A
Chemicals, Peptides, and Recombinant Proteins		
Oryzalin PESTANAL®	Sigma-Aldrich	Cat#36182-100MG
Latrunculin B from *Latruncula magnifica*	Sigma-Aldrich	Cat#L5288-1MG
Experimental Models: Organisms/Strains		
Arabidopsis: ProMAG5:MAG5-GFP *mag5-1*	Hara-Nishimura Lab., (Takagi et al., 2013)	N/A
Arabidopsis: Pro35S:SEC13A-GFP	Hara-Nishimura Lab., (Takagi et al., 2013)	N/A
Arabidopsis: Pro35S:YFP-SEC24A	Hara-Nishimura Lab., (Nakano et al., 2009)	N/A
Arabidopsis: ProUBQ10:mCherry-SYP32	Geldner Lab., (Geldner et al., 2009)	WAVE22R
Arabidopsis: Pro35S:mCherry-HDEL	Nebenführ Lab., (Nelson et al., 2007)	ER-rb
Arabidopsis: ProMAG5:MAG5-GFP ProUBQ10:mCherry-SYP32 *mag5-1*	This paper	N/A
Arabidopsis: Pro35S:SEC13A-GFP ProUBQ10:mCherry-SYP32	This paper	N/A
Arabidopsis: Pro35S:YFP-SEC24A ProUBQ10:mCherry-SYP32	This paper	N/A
Arabidopsis: ProMAG5:MAG5-GFP Pro35S:mCherry-HDEL *mag5-1*	This paper	N/A
Arabidopsis: Pro35S:SEC13A-GFP Pro35S:mCherry-HDEL	This paper	N/A
Arabidopsis: Pro35S:YFP-SEC24A Pro35S:mCherry-HDEL	This paper	N/A
Arabidopsis: ProMAG5:MAG5-mRFP *mag5-1*	This paper	N/A
Arabidopsis: Pro35S:YFP-SEC24A ProMAG5:MAG5-mRFP *mag5-1*	This paper	N/A
Arabidopsis: ProSYP32:mGFP-SYP32 ProUBQ10:mCherry-PICL TMD	This paper	N/A

Oligonucleotides		
Primer : IF-SYP32-pF : AACCAATTCAGTCGACGCTGAAGAGAGAAATCGAAAACC	This paper	N/A
Primer : IF-SYP32-pR : GCCCTTGCTCACCATTATTCTTCCTCCAATTCCTTGGA	This paper	N/A
Primer : IF-SYP32-F : GGAGGCGGAGGTGCTATGTCGGCAAGGCATGGG	This paper	N/A
Primer : IF-SYP32-3UTRR : AAGCTGGGTCTAGATATCTTTCGTCTCTGTAGTGCCT	This paper	N/A
Primer : mGFP-F : ATGGTGAGCAAGGGCGAG	This paper	N/A
Primer : mGFP-L-R : AGCACCTCCGCCTCCACCCTTGTACAGCTCGTCCATGC	This paper	N/A
Primer : IF-proUBQ10-F : AACCAATTCAGTCGACAGTCTAGCTCAACAGAGCTTTTAAC	This paper	N/A
Primer : proUBQ10-R : GGCTGTTAATCAGAAAAACTCAGA	This paper	N/A
Primer : IF-PICL-TMD-F : GGAGGCGGAGGTGCTAAAGCTGAAACATGGCATCTCA	This paper	N/A
Primer : IF-PICL-TMD-R : AAGCTGGGTCTAGATATCAATAATTTTTCCCAACAATGA	This paper	N/A
Primer : IF-proUBQ10-mCherry-F : TTCTGATTAACAGCCATGTTGAGCAAGGGCGAGG	This paper	N/A
Primer : mCherry-L-R : AGCACCTCCGCCTCCACCCTTGTACAGCTCGTCCATGC	This paper	N/A
Recombinant DNA		
Pro35S:mCherry-HDEL	Nebenführ Lab., (Nelson et al., 2007)	ER-rb
ProMAG5:MAG5-mRFP	This paper	N/A
ProSYP32:mGFP-SYP32	This paper	N/A
ProUBQ10:mCherry-PICL TMD	This paper	N/A
Software and Algorithms		
Fiji (ImageJ)	NIH, (Schindelin et al., 2012)	https://fiji.sc/
MetaMorph (ver. 7.8.3.0)	Molecular Devices	https://www.moleculardevices.co.jp/

Plant Materials and Growth Conditions

Arabidopsis thaliana, accession Columbia-0 (Col-0), was used as the wild-type plant. The following transgenic lines used in this study were described previously: ProMAG5:MAG5-GFP *mag5-1* (Takagi et al., 2013), SEC13A-GFP (Takagi et al., 2013), and YFP-SEC24A (Nakano et al., 2009). mCherry-SYP32 [WAVE22R (Geldner et al., 2009)] and mCherry-HDEL [ER-rb (Nelson et al., 2007)] were provided by Dr. N. Geldner and Dr. A. Nebenführ, respectively. Seeds were surface-sterilized with 70% ethanol and then sown onto 1x MS medium that contained 0.5% [w/v] Gellan Gum (Wako), 1% [w/v] sucrose, 1x Murashige-and-Skoog medium (Wako), and 2.5 mM MES-KOH, pH 5.7. The seeds were incubated at 4 °C for 2 d to break dormancy, followed by growth at 22 °C under continuous light.

Live Cell Imaging

Fluorescence images from cotyledon epidermal cells of 3-d-old seedlings were captured using an inverted fluorescence microscope (IX83; Olympus) equipped with a total internal reflection fluorescence microscopy system (IX2-RFAEVA-2; Olympus), solid-state lasers at 488 nm (Sapphire 488 LP; Coherent) and 561 nm (Sapphire 561 LP; Coherent), 100x oil immersion objectives (UApoN 100x OTIRF, numerical aperture (NA) = 1.49; UPlanApo 100x OHR, NA = 1.50; Olympus), Dual View 2 emission splitting system (Photometrics) and a EM-CCD camera (iXon3 897; Andor). For real-time imaging, time-sequential images were captured at 100 ms intervals for 10-20 s. Images were processed using MetaMorph (Molecular Devices) and Fiji (Schindelin et al., 2012).

Molecular Cloning

Genomic DNA of wild-type plants was used to PCR amplify the following regions: 2.0 kb of the *SYP32* upstream sequence, 2.3 kb sequence including the coding region and 3’ UTR of *SYP32*, 2.0 kb of the *UBQ10* promoter, and the C-terminal region of *PICL* (see Key Resource Table). mGFP (Segami et al., 2018) and mCherry (Shaner et al., 2004) were also amplified by PCR (see Key Resource Table). The amplified fragments were inserted into pENTER 1A dual selection (Invitrogen) using an In-Fusion HD cloning kit (Clontech) to produce the ProSYP32:mGFP-SYP32 and ProUBQ10:mCherry-PICL TMD. ProSYP32:mGFP-SYP32 and ProUBQ10:mCherry-PICL TMD were transferred into the destination vectors pBGW (Karimi et al., 2002) and pGWB601 (Nakamura et al., 2010) using LR clonase II

(Invitrogen), respectively. For the expression of MAG5-mRFP driven by the native promoter, the LR recombination reaction was performed to transfer the fragment of ProMAG5:MAG5Δstop (Takagi et al., 2013) into the destination vector pGWB653 (Nakamura et al., 2010). pFGC19/mCherry-HDEL was described previously (Nelson et al., 2007). These binary vectors were introduced into *Agrobacterium tumefaciens* (strain GV3101) by electroporation. The binary vectors were transformed into wild-type, *mag5-1* or ProMAG5:MAG5-GFP *mag5-1* plants with *Agrobacterium* using the floral dip method (Clough and Bent, 1998) to generate ProSYP32:mGFP-SYP32 ProUBQ10:mCherry-PICL-TMD, ProMAG5:MAG5-mRFP *mag5-1* or ProMAG5:MAG5-GFP Pro35S:mCherry-HDEL *mag5-1*. T1 seeds were selected in 1x MS medium containing 10 mg/L of BASTA to establish independent transgenic lines. The following transgenic lines used in this study were generated by crossing: ProMAG5:MAG5-GFP mCherry-SYP32 *mag5-1*, SEC13A-GFP mCherry-SYP32, YFP-SEC24A mCherry-SYP32, SEC13A-GFP mCherry-HDEL, YFP-SEC24A mCherry-HDEL, and YFP-SEC24A ProMAG5:MAG5-mRFP *mag5-1*.

Pharmacological Treatment

Latrunculin B and oryzalin stock solutions (5 mM and 50 mM, respectively) were made in DMSO. Three-day-old seedlings were incubated in water containing 0.3% DMSO (mock) or 10 µM latrunculin B and 50 µM oryzalin (Lat B and Oryzalin) for 1 h. The seedlings were observed immediately after the treatment.

Quantitative Analysis of Colocalization of COPII and ERES Markers

Fluorescence peaks of spots labeled with YFP-SEC24A (COPII marker) and MAG5-mRFP (ERES marker) were detected using the find maxima tool in ImageJ. To minimize detection errors, each of fluorescence spots of YFP-SEC24A was manually verified by referring to its time-sequential image. The YFP-SEC24A spot whose peak was positioned in a square region of 5 x 5 pixels (400 × 400 nm) centered at MAG5-mRFP peak was defined as colocalized.

Quantitative Analysis of Free ERESs and Golgi-Associated ERESs

Fluorescence peaks of ERES (MAG5-GFP) spots were detected using the find maxima tool in ImageJ (Figure S2A and S2D). The regions of the Golgi stacks were segmented from the original fluorescence images by applying Gaussian blurring followed by binarization using an automatic thresholding method (Figure S2B and

S2C). The ERES spots whose peaks were positioned in the Golgi-stack regions were defined as Golgi-associated ERESs, and the other spots were defined as free ERESs (Figure S2D). Taking into account the possibility that ERES spots may overlap each other, the ratio of free and Golgi-associated ERESs was measured after correcting each number by the average signal intensity of the ERES peak.

For quantification of dynamic relationship of ERESs with Golgi stacks, frequency of ERES capture and release events by a Golgi stack in 20 s was manually counted from time-sequential images obtained at 100 ms intervals for 20 s.

Quantitative Analysis of Free ERESs on the ER Subdomains

Punctate ERESs and ER structures such as ER tubules and ER sheets were extracted from fluorescence microscopy images by semi-automatic image processing techniques consist of several morphological processing steps (Haralick et al., 1987). Details of the image processing protocol to quantify the topological relationship between punctate ERESs and ER are described in Figure S3.

The image processing procedure for extraction of the ER sheet structure is as follows: The original image was Gaussian-blurred [Figure S3C(2)] followed by contrast enhancement based on white top-hat transform through rotational morphological processing (RMP) [Figure S3C(3)]. This enhanced image was binarized by an automatic thresholding method [Figure S3C(4)]. The sheet regions were extracted by applying the opening procedure with RMP to the binarized image [Figure S3C(5)] followed by area opening operation to remove small isolated regions [Figure S3C(6)]. The ER body region was manually removed [Figure S3C(7)]. The ER sheet grooves were extracted by black top-hat transform through RMP [Figure S3C(8)] followed by binarization and area opening operation [Figure S3C(9)]. The ER sheet structure was extracted by subtracting the ER sheet grooves from the ER sheet regions [Figure S3C(10)].

The image processing procedure for extraction of the ER tubule region is as follows: The original image was Gaussian-blurred [Figure S3D(2)] followed by contrast enhancement based on white top-hat transform through RMP [Figure S3D(3)]. This enhanced image was binarized by an automatic thresholding method [Figure S3D(4)] followed by area opening operation [Figure S3D(5)]. The tubule regions were extracted by subtracting the ER sheet region from this binarized image [Figure S3D(6)] followed by area opening operation [Figure S3D(7)].

The image processing procedure for extraction of the punctate ERESs is as follows: The original image was Gaussian-blurred [Figure S3E(2)] followed by closing through RMP [Figure S3E(3)] and binarization by an automatic thresholding method [Figure S3E(4)]. The punctate ERESs were extracted from the original image [Figure S3E(1)] using the find maxima tool in ImageJ. The beaded rings of ERESs (Golgi-associated ERESs) were manually extracted [Figure S3E(5)], and the other punctate ERESs were defined as Golgi-free ERESs.

Motility Analysis

Trajectories of free ERESs, Golgi-associated ERESs, and Golgi stacks were manually extracted from time-sequential images captured at 100 ms intervals for 20 s using Manual Tracking plugin of ImageJ. Time-coded trajectories of the fluorescence particles were tracked from the center of each two-dimensional lattice.

Accession Numbers

Sequence data from this article can be found in The *Arabidopsis* Information Resource (TAIR) (http://www.arabidopsis.org) with the accession numbers as follows: *MAG5/SEC16A*, At5g47480; *SEC13A*, At3g01340; *SEC24A*, At3g07100; *SYP32*, At3g24350; *PICL*, At1g05320; *UBQ10*, At4g05320.

Supplemental References

Clough, S.J., and Bent, A.F. (1998). Floral dip: a simplified method for *Agrobacterium*-mediated transformation of *Arabidopsis thaliana*. Plant J. *16*, 735-743.

Geldner, N., Denervaud-Tendon, V., Hyman, D.L., Mayer, U., Stierhof, Y.D., and Chory, J. (2009). Rapid, combinatorial analysis of membrane compartments in intact plants with a multicolor marker set. Plant J. *59*, 169-178.

Haralick, R.M., Sternberg, S.R., and Zhuang, X. (1987). Image analysis using mathematical morphology. IEEE Trans. Pattern Anal. Mach. Intell. *9*, 532-550.

Karimi, M., Inze, D., and Depicker, A. (2002). GATEWAY vectors for *Agrobacterium*-mediated plant transformation. Trends Plant Sci. *7*, 193-195.

Nakamura, S., Mano, S., Tanaka, Y., Ohnishi, M., Nakamori, C., Araki, M., Niwa, T., Nishimura, M., Kaminaka, H., Nakagawa, T.*, et al.* (2010). Gateway binary vectors with the bialaphos resistance gene, *bar*, as a selection marker for plant transformation. Biosci. Biotechnol. Biochem. *74*, 1315-1319.

Nakano, R.T., Matsushima, R., Ueda, H., Tamura, K., Shimada, T., Li, L., Hayashi, Y., Kondo, M., Nishimura, M., and Hara-Nishimura, I. (2009). GNOM-LIKE1/ERMO1 and SEC24a/ERMO2 are required for maintenance of endoplasmic reticulum morphology in *Arabidopsis thaliana*. Plant Cell *21*, 3672-3685.

Nelson, B.K., Cai, X., and Nebenfuhr, A. (2007). A multicolored set of *in vivo* organelle markers for co-localization studies in Arabidopsis and other plants. Plant J. *51*, 1126-1136.

Schindelin, J., Arganda-Carreras, I., Frise, E., Kaynig, V., Longair, M., Pietzsch, T., Preibisch, S., Rueden, C., Saalfeld, S., Schmid, B.*, et al.* (2012). Fiji: an open-source platform for biological-image analysis. Nat. Methods *9*, 676-682.

Segami, S., Tomoyama, T., Sakamoto, S., Gunji, S., Fukuda, M., Kinoshita, S., Mitsuda, N., Ferjani, A., and Maeshima, M. (2018). Vacuolar H(+)-Pyrophosphatase and Cytosolic Soluble Pyrophosphatases Cooperatively Regulate Pyrophosphate Levels in *Arabidopsis thaliana*. Plant Cell *30*, 1040-1061.

Shaner, N.C., Campbell, R.E., Steinbach, P.A., Giepmans, B.N., Palmer, A.E., and Tsien, R.Y. (2004). Improved monomeric red, orange and yellow fluorescent proteins derived from *Discosoma* sp. red fluorescent protein. Nat. Biotechnol. *22*, 1567-1572.

Takagi, J., Renna, L., Takahashi, H., Koumoto, Y., Tamura, K., Stefano, G., Fukao,

Y., Kondo, M., Nishimura, M., Shimada, T.*, et al.* (2013). MAIGO5 functions in protein export from Golgi-associated endoplasmic reticulum exit sites in *Arabidopsis*. Plant Cell *25*, 4658-4675.